TOWARDS ON-BOARD IDENTIFICATION OF SPACE SYSTEMS

Virtual Conference 19–23 October 2020

Olga-Orsalia Christidi-Loumpasefski[1], David Nguyen[2], Kostas Nanos[1], Georgios Rekleitis[1], Iosif S. Paraskevas[1], Yves-Julien Regamey[2], Antoine Verhaeghe[2], Davide Casu[3], Evangelos Papadopoulos[1] and Finn Ankersen[4]

[1]*National Technical University of Athens, School of Mechanical Engineering, Control Systems Lab, (Heroon Polytechniou 9, Zografos, Attica, Greece, {olgachr, knanos}@central.ntua.gr, georek@gmail.com, isparas@mail.ntua.gr, egpapado@central.ntua.gr)*

[2]*Centre Suisse d'Electronique et Microtechnique (Rue Jaquet-Droz 1, 2002 Neuchâtel, Switzerland, {david.nguyen, yves-julien.regamey, antoine.verhaeghe}@csem.ch)*

[3]*Thales Alenia Space - France (5 Allée des Gabians, 06150 Cannes, France, davide.casu@thalesaleniaspace.com)*

[4]*European Space Agency, ESTEC (Noordwijk, the Netherlands, Finn.Ankersen@esa.int)*

ABSTRACT

To enhance current robotic OOS capabilities, autonomous operations must be considered, that will rely on advanced controllers. The design and adaptation of such controllers requires reliable system identification methods and algorithms, especially regarding the system inertial parameters and flexibilities. The main objective of the OBSIdian project is the development and application of System Identification (SYSID) methodologies based on appropriate formulations of system dynamics and the subsequent development and application of appropriate identification algorithms. This will result in the development of an on-board computational efficient and reliable software for SYSID.

1 INTRODUCTION

In the future, missions focusing on the construction of large systems on-orbit, servicing of existing space assets, or end-of-life disposal of satellites from valuable GEO locations will proliferate. These tasks fall under the broad terms of On-Orbit Servicing (OOS) and On-Orbit Assembly, the importance of which is generally accepted by both space agencies and the private sector investing in space.

A cost-effective way to tackle these challenges is to use Space Manipulator Systems (SMS). To enhance current OOS capabilities, autonomous operations must be considered, that will rely on advanced controllers. The design and adaptation of such controllers require reliable system identification methods, especially regarding the system inertial parameters and flexibilities.

The main objective of the OBSIdian project is the development and application of System Identification (SYSID) methods based on appropriate formulations of system dynamics and the subsequent development and application of appropriate identification techniques/ algorithms. This will result in the development of an on-board computational efficient and reliable software for SYSID with the purpose of generating corrective models and eventually controllers, when these models cannot be predicted reliably by computational models (due to uncertainties, non-linearities, un-modelled dynamics etc.), or by scaled (i.e. scaling difficulties) or lab experiments (e.g. sloshing). Model validation and verification strategies are also OBSIdian's objectives. The OBSIdian mission scenario lies on a basic OOS concept, which includes a servicing Chaser satellite equipped with a manipulator, and a Target satellite; fuel sloshing effects and flexible appendages are taken into consideration, see Figure 1.

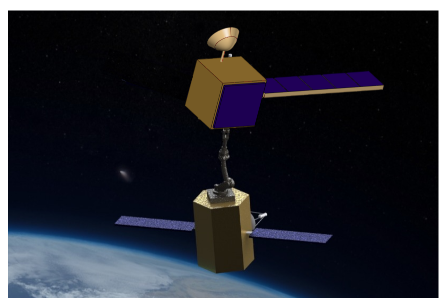

Figure 1: A target satellite mated with a chaser satellite using a manipulator.

Specifically, the OBSIdian project focuses on the SYSID during two distinct OOS specific phases. The first phase takes place before any contact with the Target satellite, during which the Chaser performs internal SYSID tasks with the goal being to identify with high accuracy the necessary values of its own system parameters. If the Target is cooperative, it may perform similar tests on itself, in order to transmit updated data to the Chaser. However, from the SYSID point of view, the same methods to those for the

Chaser can be used. The second phase takes place after the Target rigid capture by the Chaser's manipulator during berthing. Here the aim is to identify with high accuracy the system parameters of the rigidly mated full system. Note that both experimental (i.e. inputs specifically designed for identification) and operational (i.e. regular inputs applied during operations) SYSID methods are considered.

To evaluate the performance of the various developed identification methods and algorithms, and observe the associated requirements, as well as their advantages and disadvantages during the identification of various types of uncertain parameters (i.e. inertial parameters, sloshing model parameters and flexible appendages modal parameters), several Benchmark Problems have been envisioned. Thus, one of the outcomes of these tests will be the trade-off analysis and choice of the most efficient methods and algorithms. Subsequently, these methods and algorithms will be employed in more realistic cases, namely the Study Cases, in which all the studied types of uncertainties are simultaneously taken into account.

In this paper, the Benchmark Problems will be described briefly and partially, focusing on the (planar initially) models, the identification methods (proposed or developed by the authors) for each Benchmark Problem and some of the identification algorithms used. As the project is still ongoing, preliminary results on Benchmark Problems will be presented.

2 IDENTIFICATION ALGORITHMS

In OBSIdian, in case of lumped models such as the spacecraft (S/C) rigid body and the sloshing model, *parametric identification* is considered. Moreover, in case of continuous models such as flexible appendages, *modal analysis* algorithms will be used.

2.1 Parametric Identification

To employ some of the parametric identification algorithms, specifically least squares algorithm and its modifications, such as Instrumental Variables (IV) and Total Least Squares (TLS), the model dynamics must be expressed linearly with respect to a minimal (of minimum dimension) vector of parameters $\boldsymbol{\alpha}$:

$$\mathbf{Y}\boldsymbol{\alpha} = \mathbf{b} \tag{1}$$

where $\mathbf{Y}$ is the regressor matrix which contains only measurable quantities, and $\mathbf{b}$ is a vector which contains only known or measurable quantities.

In this paper, parametric identification based on the promising IV, TLS, and Unscented Kalman Filter (UKF) algorithms will be presented.

2.1.1 Total Least Squares (TLS)

The TLS is ideally suited for situations in which all data are corrupted by noise, which is almost always the case in engineering applications. Specifically, the Singular Value Decomposition (SVD) of [**Y b**] can be used to find a unique solution:

$$[\mathbf{Y} \quad \mathbf{b}] = \mathbf{U}\boldsymbol{\Sigma}\mathbf{V}^{\mathrm{T}} = \mathbf{U}\boldsymbol{\Sigma}\begin{bmatrix} \mathbf{V}_{pp} & \boldsymbol{\upsilon}_{pq} \\ \boldsymbol{\upsilon}_{qp} & \upsilon_{qq} \end{bmatrix}^{\mathrm{T}} \tag{2}$$

Hence, the TLS solution for $\boldsymbol{\alpha}$ is obtained as [1]:

$$\boldsymbol{\alpha} = -\boldsymbol{\upsilon}_{pq}\upsilon_{qq}^{-1} \tag{3}$$

2.1.2 Instrumental Variables (IV)

The IV algorithm deals with noisy regressor matrices and proposes to build an appropriate instrument matrix $\mathbf{V}$. The IV solution for $\boldsymbol{\alpha}$ is obtained as:

$$\boldsymbol{\alpha} = (\mathbf{V}^T\mathbf{Y})^{-1}\mathbf{V}^T\mathbf{b} \tag{4}$$

A classical solution is to build $\mathbf{V}$ from simulated data $\mathbf{q}_s, \dot{\mathbf{q}}_s, \ddot{\mathbf{q}}_s$ instead of measured data, [2]. The iterative procedure adopted [2], is presented in Figure 2.

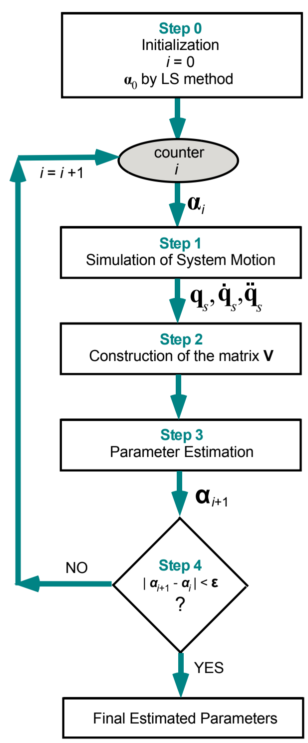

Figure 2: The flowchart of the IV algorithm.

2.1.3 Unscented Kalman Filter (UKF)

In UKF, a state-space formulation of a linear/ nonlinear system dynamics is considered,

$$\dot{\mathbf{x}}(t) = \mathbf{f}(\mathbf{x}(t), \mathbf{u}(t)) \tag{5}$$

where $\mathbf{x}(t)$ is the extended state vector consisting of both the states and system parameters to be estimated, and $\mathbf{u}(t)$ is the input.

Moreover, the general form of the dynamic equations of the systems under study in this paper is,

$$\mathbf{H}\ddot{\mathbf{q}} + \mathbf{C} = \mathbf{Q} \tag{6}$$

where $\mathbf{H}$ is system inertia matrix, vector $\mathbf{C}$ contains the remaining terms, and $\ddot{\mathbf{q}}$, $\mathbf{Q}$ are the vectors of generalized accelerations and forces of the system, respectively. In this case, and considering constant vector of parameters $\boldsymbol{\alpha}$ over time,

$$\dot{\mathbf{x}}(t) = \begin{bmatrix} \dot{\mathbf{q}}(t) \\ \ddot{\mathbf{q}}(t) \\ \dot{\boldsymbol{\alpha}} \end{bmatrix} = \begin{bmatrix} \mathbf{x}(2)(t) \\ \mathbf{H}^{-1}(\mathbf{x}(t))(\mathbf{Q}(t) - \mathbf{C}(\mathbf{x}(t))) \\ \mathbf{0} \end{bmatrix} \tag{7}$$

2.2 Modal Analysis

Modal analysis makes use of measurements to estimate modal parameters, consisting of modal frequencies, damping ratios, mode shapes and modal participation factors. Two main classifications are the most common.

The first classification is between Experimental (EMA) and Operational (OMA) Modal Analysis. In EMA, the excitation for the identification process is a user choice, while in OMA, the excitation is the one applied during a specific operation. The second classification is between identification algorithms that use data in the time domain (TD) and those that use data in the frequency domain (FD). The measured data can be in the form of either Frequency Response Functions (FRFs) for FD algorithms or impulse responses for TD algorithms.

In this paper, identification results based on the promising modal analysis algorithms Least Square Complex Exponential (LSCE), Rational Fraction Polynomial (RFP), Covariance-driven Stochastic Subspace Identification (SSI-COV) and Data-driven Stochastic Subspace Identification (SSI-DATA) will be presented in a set of simulations.

3 IDENTIFICATION METHODOLOGIES FOR SPACE SYSTEMS

3.1 Inertial Parameter Identification

Inertial parameter identification methods can be classified as vision-based [3]-[4], as those that use equations of motion [5]-[6], and as momentum-based, [5], [7]-[9]. The vision-based methods are applicable in the pre-capture phase and they can identify only some satellite's inertial parameters. The methods based on the equations of motion are sensitive to sensor noise since they require noisy acceleration measurements. Momentum-based methodologies do not require acceleration measurements and subsequently, they are less sensitive to sensor noise. Hence, they can be considered as the most promising methods for inertial parameter identification.

3.2 Identification of Flexible Appendages

The problem of parameter estimation for flexible components is particularly well studied for structural applications such as those in civil engineering; examples of spacecraft applications exist as well. On-orbit identification experiments of structural modal parameters have been implemented on some spacecrafts such as the Hubble Space Telescope (HST) [10], the Galileo spacecraft [11], and the Engineering Test Satellite VIII (ETS-VIII), [12]. In [13], accelerometer data from the ROSA flight experiment on ISS were analyzed in an attempt to identify the ROSA system modal parameters.

3.3 Identification of Sloshing

Fuel sloshing disturbs the satellite motion especially when fast maneuvers are required, and particularly when large fuel tanks are employed. To represent the fuel sloshing dynamics, two equivalent models are mainly used in the literature: the pendulum and the mass-spring-damper models, [10]. In [15] the pendulum equivalent model has been adopted and the effects of fuel sloshing on the inertial parameter identification of on-orbit manipulators has been addressed. However, none of the sloshing parameters has been estimated explicitly. To identify the pendulum model parameters, experiments using a full-scale model of a flight tank were conducted [16], and a Kalman filter technique has been used [17]. However, to the best of the authors' knowledge, there is lack of methodologies for the estimation of mass-spring-damper sloshing model parameters.

4 BENCHMARK PROBLEMS

The Benchmark Problems (BPs) are developed in order to test the various parametric identification and modal analysis algorithms in simplified (planar) models, in the presence of various types of uncertain parameters (i.e. inertial parameters, sloshing model parameters and flexible appendages modal parameters). Thus, one of the outcomes of these tests will be the final trade-off analysis and choice of the methods to be used in the more realistic Study Cases, in which all the studied types of uncertainties will be taken into account.

Three BPs are envisioned, each one addressing the identification of a separate type of uncertainty.

4.1 Benchmark Problem 1: Inertial Parameters

In Benchmark Problem 1 (BP1), see Table I, the planar model of a single-manipulator space robot is envisioned, and its inertial parameters are identified. Two sub-problems are distinguished: BP1A with a free-floating space robot (i.e. no actuation on the S/C base), and BP1B with a fully actuated free-flying space robot (i.e. active thrusters and reaction wheels on the S/C base). No sloshing effects or flexible appendages are included in both cases.

Table I. Benchmark Problems 1: Inertial Parameters

Benchmark Problem 1A (BP1A)	Benchmark Problem 1B (BP1B)
Identification of inertial parameters	
Experimental parametric identification	
Model: 2D *free-floating* space robot	**Model**: 2D *free-flying* space robot

As it can be seen from Table I, BP1 implements Experimental Identification, in the sense that the excitation of the system is the user's choice, as it fits best the needs of the identification process. Furthermore, BP1 employs parametric identification methods. In this paper, BP1A is presented.

4.1.1 BP1A: Free-Floating Case

4.1.1.1 System Model

The dynamics of a planar 2-DoF single-manipulator SMS in free-floating mode, see Figure 3, is given by (6) where $\mathbf{Q}=[0\ \ \tau_1\ \ \tau_2]^{\mathrm{T}}$ and

$$\ddot{\mathbf{q}} = [\ {}^{0}\dot{\omega}_{0z}\quad \ddot{\theta}_1\quad \ddot{\theta}_2\ ]^{\mathrm{T}} \tag{8}$$

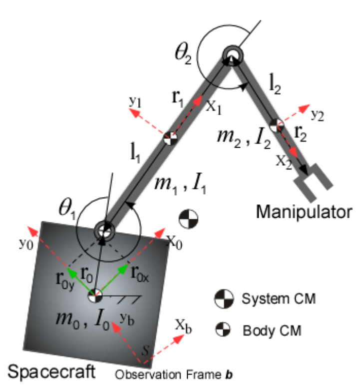

Figure 3: A SMS with a single 2-DoF manipulator.

where $\dot{\omega}_{0z}$ is the S/C angular acceleration, and $\ddot{\theta}_1, \ddot{\theta}_2$ τ_1, τ_2 are the manipulator's joint accelerations and torques, respectively. Moreover, **H**, **C** are given in [9].

The system angular momentum h_{cm} expressed in the inertial frame is given by:

$$h_{cm} = D\,{}^{0}\omega_{0z} + \mathbf{D}_q\,\dot{\boldsymbol{\theta}} \tag{9}$$

where D, $\mathbf{D}_q$ are inertia-type quantities given in [9] and $\dot{\boldsymbol{\theta}} = [\ \dot{\theta}_1\quad \dot{\theta}_2\ ]^{\mathrm{T}}$.

4.1.1.2 Parameter Identification Equations

To identify free-floating system inertial parameters, the *Angular Momentum Conservation approach* (AMC), which is based on the conservation of angular momentum of a space manipulator system in free-floating mode [9], and the *Dynamic Equation approach* (DE) which is based on the system equations of motion, are applied.

In AMC approach, the system angular momentum seen in Eq. (9), is reformulated as in (1):

$$\mathbf{Y}_h\left(\dot{\theta}_1, \dot{\theta}_2, \theta_1, \theta_2, {}^{0}\omega_{0z}\right)\boldsymbol{\alpha} = h_{cm} \tag{10}$$

and in DE approach, the system equations of motion, (6), are written as in (1):

$$\mathbf{Y}_\tau\left({}^{0}\dot{\omega}_{0z}, {}^{0}\omega_{0z}, \ddot{\theta}_1, \ddot{\theta}_2, \dot{\theta}_1, \dot{\theta}_2, \theta_1, \theta_2\right)\boldsymbol{\alpha} = \mathbf{Q} \tag{11}$$

Note that in both equations, the set of inertial parameters $\boldsymbol{\alpha}$ is the same and consists of parameters that are combinations of S/C and manipulator's links inertial parameters, and is given in detail in [18].

4.1.1.3 Inputs and Required Measurements

System inputs consist of the joint torques acting on the manipulator joints. As it can be seen by (10), the measurements required for SYSID based on AMC are the S/C angular velocity and the arm joints angles, rates. Furthermore, as it can be seen in (11), SYSID based on DE additionally requires the S/C angular acceleration, and the arm joints accelerations.

Hence, the required sensors for BP1A are the Inertial Measurement Unit (IMU) and the manipulator joint-motor encoders. The angular rate error is selected as white noise with a typical value of Angular Random Walk (ARW) equal to $0.09\,^{\circ}/\sqrt{h}$.

4.1.1.4 Parameters and Excitation

System parameters for B1 are shown in Table II.

Table II. Parameters of the planar free-floating SMS.

Body	l_i (m)	r_i (m)	m_i (kg)	I_i (kg m^2)
0	-	$[0.99\ 0.99]^T$	400	66.67
1	1.9	0.168	12.1	17.27
2	1.73	0.168	11.7	14.10

The selected exciting trajectories of arm joints are based on truncated Fourier series, [9] and h_{cm}=68 *Nms*.

4.1.1.5 Identification Results

The Relative Errors (RE) resulted from the application of the TLS, IV and UKF algorithms using the AMC and DE approaches are shown in Table III and Table IV, respectively. Note that the UKF algorithm is applied only based on DE since its application requires the use of system equations of motion. As it can be seen from Table III and Table IV, the TLS and IV yield comparable results. In the DE approach, UKF yields better estimates than TLS and IV; however, its performance depends strongly on filter parameter tuning and initial knowledge of system inertial parameters, e.g. here, it was taken as 55%α. Moreover, and most importantly, the AMC approach guarantees better estimates than the DE approach since, as mentioned above, it is less sensitive to sensor noise as it does not require acceleration measurements.

Table III. B1A TLS, IV, UKF relative errors (RE) based on Angular Momentum Conservation approach.

Parameter	TLS RE (%)	IV RE (%)	UKF RE (%)
$\alpha(1)$	0.09	0.09	-
$\alpha(2)$	0.28	0.28	-
$\alpha(3)$	0.25	0.25	-
$\alpha(4)$	0.57	0.57	-
$\alpha(5)$	0.18	0.18	-
$\alpha(6)$	0.10	0.10	-
$\alpha(7)$	0.38	0.38	-
$\alpha(8)$	0.02	0.02	-

Table IV. B1A TLS, IV, UKF Relative Errors (RE) based on Dynamic Equation approach.

Parameter	TLS RE (%)	IV RE (%)	UKF RE (%)
$\alpha(1)$	12.67	8.16	0.28
$\alpha(2)$	18.46	17.44	0.74
$\alpha(3)$	5.53	5.23	3.66
$\alpha(4)$	13.67	18.15	10.05
$\alpha(5)$	17.31	14.64	13.77
$\alpha(6)$	8.03	4.50	0.00
$\alpha(7)$	4.49	5.54	8.22
$\alpha(8)$	2.95	1.64	8.19

4.2 Benchmark Problem 2: Sloshing Parameters

In BP2, see Table V, the planar model of a satellite in the presence of sloshing effect is envisioned. In this paper, a preliminary model in 1D is considered. The satellite parameters are assumed known and sloshing model parameters are identified.

As it can be seen from Table V, BP2 implement Experimental Identification. Furthermore, BP2 employ parametric identification methods.

Table V. Benchmark Problem 2: Sloshing Parameters.

Benchmark Problem 2 (BP2)
Identification of sloshing model parameters
Experimental parametric identification
Model: 2D satellite and 2D sloshing model

4.2.1 Preliminary 1D Model

To study the effect of the fuel sloshing mass on the S/C, the S/C mass m_0 and the sloshing mass m_s are considered as a 2-DoF mass-spring-damper with spring and damping constants k_s, c_s respectively, as shown in Figure 4.

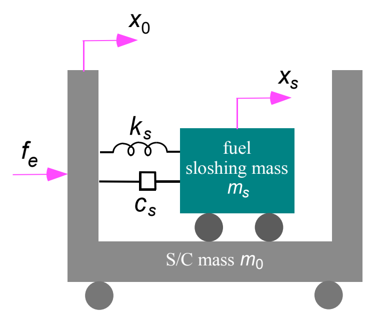

Figure 4: A 2-DoF sloshing mass-spring-damper model.

The equations of motion for the S/C and the sloshing mass are:

$$m_0\ddot{x}_0 + k_s(x_0 - x_s) + c_s(\dot{x}_0 - \dot{x}_s) = f_e \tag{12}$$

$$m_s\ddot{x}_s - k_s(x_0 - x_s) - c_s(\dot{x}_0 - \dot{x}_s) = 0 \tag{13}$$

where f_e is the force applied to the S/C, and $x_0, \dot{x}_0, \ddot{x}_0$ and $x_s, \dot{x}_s, \ddot{x}_s$ are the position, velocity, acceleration of S/C and sloshing fuel Center of Mass (CoM), respectively.

4.2.2 Parameter Identification Equations

To identify the sloshing model parameters in the preliminary 1D sloshing model presented, the following methodology is developed.

Considering the S/C velocity as the system's output, the system transfer function is given by,

$$G(s) = \frac{\dot{x}_0}{f_e} = \frac{1}{m_0}\frac{s^2 + (c_s/m_s)s + k_s/m_s}{s(s^2 + c_s^* s + k_s^*)} \tag{14}$$

where

$$k_s^* = k_s\frac{m_0 + m_s}{m_0 m_s} \quad \text{and} \quad c_s^* = c_s\frac{m_0 + m_s}{m_0 m_s} \tag{15}$$

Eq. (14) can be written in the time domain. Moreover, considering the S/C CoM acceleration $\ddot{x}_0$ as the measurable quantity and by integrating twice to avoid the differentiation of noisy signals, (14) is given by,

$$\ddot{x}_0 + c_s^* \dot{x}_0 + k_s^* x_0 = \\ = \frac{1}{m_0} F_s + \frac{c_s}{m_0 m_s} \int_0^t F_s \, dt + \frac{k_s}{m_0 m_s} \int_0^t \int_0^t F_s \, dt \quad (16)$$

The equation of motion (16) for the S/C is written linearly with respect to the set of sloshing model parameters $\boldsymbol{\alpha}_s$ i.e. in formulation of (1), as follows:

$$\mathbf{Y}_s\left(x_0, \dot{x}_0, f_e\right)\boldsymbol{\alpha}_s = b_s(F_e, \ddot{x}_0) \quad (17)$$

where

$$\boldsymbol{\alpha}_s = \begin{bmatrix} c_s^* & k_s^* & \frac{c_s}{m_0 m_s} & \frac{k_s}{m_0 m_s} \end{bmatrix}^{\mathrm{T}} \quad (18)$$

Based on (18), the estimated sloshing model parameters m_s, k_s, c_s can be derived easily.

4.2.3 Inputs and Required Measurements

The system input is the force f_e applied to the S/C by the thrusters. Additionally, as it can be seen in (17), in the 1D version of B2, the measurements required for SYSID are the S/C CoM position, velocity and acceleration. Hence, the required sensor for B2 is the IMU. Moreover, fusing GNSS, inertial, and magnetometer data may yield more accurate S/C position and velocity measurements. The selected acceleration error is white noise with a typical value of velocity random walk equal to $0.008\,(m/s)/\sqrt{h}$. Note that the state of the sloshing mass cannot be measured.

4.2.4 Parameters and Excitation

To illustrate the proposed methodology, a satellite of mass m_0=1004.5 *kg* is considered. The true values of the sloshing parameters are shown in Table VI.

The applied thruster force is a sinusoidal signal of amplitude 44 *N* and frequency 0.01 *Hz*.

4.2.5 Identification Results

The relative errors (RE) of estimated parameters by TLS and IV algorithms are shown in Table VI. UKF results are not included since its implementation indicated the possibility of observability issues.

Table VI. BP2 relative errors (RE) based on IV, TLS

Parameter	True Value	TLS RE (%)	IV RE (%)
m_s	28.7	2.44	1.86
k_s	0.16	1.08	3.14
c_s	0.03	348.84	324.87

Although the relative errors for the parameters m_s and k_s are quite low, the relative error for parameter c_s is large in both algorithms. However, as it can been seen from Figure 5, the effect of this error in satellite response is negligible. Figure 5 shows the relative error between the predicted satellite response e.g. x_0, based on the estimated parameters and the "true" satellite response.

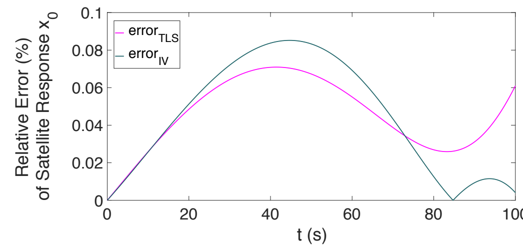

Figure 5: The RE between predicted and "true" x_0.

4.3 Benchmark Problem 3: Modal Parameters

In Benchmark Problem 3 (BP3), see Table VII, a rotating rigid hub with a flexible appendage mounted on a fixed revolute joint is envisioned, and the modal parameters of the flexible appendage are identified. Two sub-problems are envisioned: BP3A based on EMA and BP3B based on OMA.

Table VII. Benchmark Problem 3: Modal Parameters

Benchmark Problem 3A (BP3A)	Benchmark Problem 3B (BP3B)
Identification of appendages modal parameters	
EMA	**OMA**
Model: 2D flexible appendage on hub	

4.3.1 System Model

In BP3, the dynamics of a rotating rigid hub with a flexible appendage, see Figure 6, can be given by (6) where $\mathbf{Q}$=[1 0 0]$^{\mathrm{T}}$ u and

$$\ddot{\mathbf{q}} = [\ \ddot{\theta}_0 \quad \ddot{\delta}_1 \quad \dots \quad \ddot{\delta}_n\ ]^{\mathrm{T}} \quad (19)$$

where $\ddot{\theta}_0$ is the hub angular acceleration, $\ddot{\delta}_1,\ldots\ddot{\delta}_n$ are the n modal accelerations, where n is the number of dominant modes, and u is the torque applied on hub.

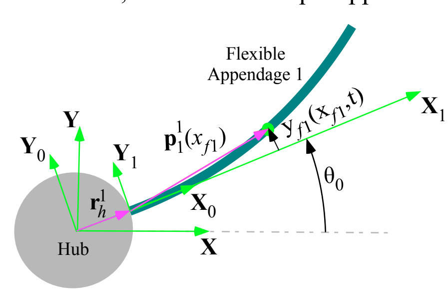

Figure 6: A planar "appendage on hub" model.

Moreover, vector **C** is given by

$$\mathbf{C} = \mathbf{D}\dot{\mathbf{q}} + \mathbf{K}\mathbf{q} \tag{20}$$

where **K**, **D** are the damping and stiffness matrices.

4.2.3 Inputs and Required Measurements

The system input in B3 is the torque applied on the hub by a motor. Moreover, in B3 the measurements required for SYSID are the acceleration of a selected number of appendage points. Hence, the required sensors for B3 are a number of accelerometers mounted on the appendage. In this work, the flexible appendage is equipped with 10 equally spaced sensors.

The noise model assumed is a zero-mean gaussian white noise. The accelerometers in the simulations are the QA2000 from Honeywell.

4.3.2 BP3A: Experimental Modal Analysis

4.3.2.1 Parameters and Excitation

The B3 system's natural frequencies and damping ratios are shown in Table VIII and the mode shapes are plotted in Figure 7.

Table VIII. B3 Natural frequencies and damping ratios

Parameter	I_{hub} ($kg\ m^2$)	fn_1 (Hz)	fn_2 (Hz)	ζ_{n1}	ζ_{n1}
	200	118.58	743.19	0.1	0.05

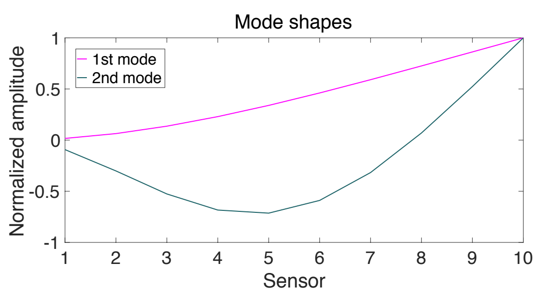

Figure 7: B3 first two mode shapes.

Furthermore, EMA methods estimate system modal parameters based on known artificial excitation. In this work, a rectangular signal is used, composed of a first step from 0 *Nm* to 2 *Nm* at t=0 *s*, followed by an opposite step from 2 *Nm* to 0 *Nm* at t=1 *s*. The duration is 5 *s*. Between 1 *s* and 5 *s*, the input is zero.

4.3.2.2 Identification Results

The relative errors based on EMA of the estimated natural frequencies and damping ratios, and the MAC value for estimated mode shapes are presented in Table IX and Table X, respectively.

The LSCE identifies accurately natural frequencies, but not all damping ratios. Other excitations may yield better results. The RFP and SSI-DATA perform very well here. The SSI-COV is capable in identifying the modal parameters even if the assumption of zero-mean white noise input is violated. However, the input signal needs to be chosen such that it does not influence the real modes in their frequential vicinity.

As it can be seen in Table IX, SSI-COV perform better than the other algorithms in the studied case.

Table IX. BP3A relative errors (RE) based on EMA

Parameter	LSCE RE(%)	RFP RE(%)	SSI_COV RE (%)	SSI_DATA RE (%)
f_{n1}	0.77	0.50	0.02	0.06
f_{n2}	0.26	0.11	0.00	0.01
ζ_{n1}	1.65	0.46	0.02	0.37
ζ_{n2}	8.48	0.97	0.03	0.69

Table X. BP3A MAC value based on EMA

Mode	LSCE MAC	RFP MAC	SSI_COV MAC	SSI_DATA MAC
1st mode	1.00	0.99	1.00	1.00
2nd mode	1.00	0.99	1.00	1.00

4.3.3 BP3B: Operational Modal Analysis

4.3.3.1 Parameters and Excitation

The parameters in BP3B are the same as in BP3A. In contrast to EMA methods, OMA methods are based on the excitation induced by the operational tasks, which in general is more conservative than the artificial. In this paper, an operational task is considered where the hub needs to be rotated for an angle of 5° every 1 *s*. The simulation time is 5 *s* as for the EMA case. This means that the setpoint (which is the desired hub angle) is composed of the addition of 5 delayed step functions of 0.5° of amplitude. A simple PID controller is implemented to compute the required joint torque to follow each new setpoint.

4.3.3.2 Identification Results

The relative errors based on OMA of the estimated natural frequencies and damping ratios, and the MAC value for estimated mode shapes are presented in Table IX and Table X, respectively.

The LSCE seems to be working with our OMA case, even though it is an EMA method. One possible explanation is that our chosen OMA excitation is a series of (escalating) step input commands, which are realized with PID-control induced torques. This excitation, though, is close to the (ideal for LSCE) impulse inputs. The RFP and SSI-DATA perform very well in the presented case. The SSI-COV yields low errors in the presented case, lower than all the other algorithms tested here, as can be seen in Table XI.

Table XI. BP3B relative errors (RE) based on OMA

Para-meter	LSCE RE(%)	RFP RE(%)	SSI_COV RE (%)	SSI_DATA RE (%)
f_{n1}	0.05	0.12	0.01	0.05
f_{n2}	0.04	0.01	0.00	0.01
ζ_{n1}	0.05	1.27	0.01	0.63
ζ_{n2}	1.15	0.33	0.01	0.56

Table XII. BP3B MAC value based on OMA

Mode	LSCE MAC	RFP MAC	SSI_COV MAC	SSI_DATA MAC
1st mode	0.99	1.00	1.00	1.00
2nd mode	1.00	0.99	1.00	0.99

5 CONCLUSION

The main objective of OBSIdian is the development and application of system identification (SYSID) methods for space systems. This will result in the development of an on-board computational efficient and reliable software for SYSID. To evaluate the performance of the various identification methods and algorithms, several Benchmark Problems (BPs) have been envisioned. In this paper, the BPs were briefly described, focusing on the (planar initially) models, the identification methods for each Benchmark Problem, and some of the identification algorithms used. As the project is still ongoing, preliminary results on Benchmark Problems were presented.

ACKNOWLEDGMENTS

This work is supported by the European Space Agency (ESA), through the project On-Board System Identification for Uncertainty Modelling & Characterization (OBSIdian), Contract Number: 4000126266/18/NL/GLC.

REFERENCES

[1] Total Least Squares, *CourseNotes, (Fall 2017) CEE 629. System Identification*, *Duke University*.

[2] Janot A, Vandanjon PO and Gautier M (2009) "Identification of robots dynamics with the instrumental variable method. In: *Proceedings of 2009 IEEE international conference on robotics and automation (ICRA)*, Kobe, Japan, pp.1762-1767.

[3] Hillenbrand U and Lampariello R (2005) Motion and parameter estimation of a free-floating space object from range data for motion prediction. In: *Proceedings of 2005 i-SAIRAS*, Munich, Germany.

[4] Aghili F (2012) A prediction and motion-planning scheme for visually guided robotic capturing of free-floating tumbling objects with uncertain dynamics. *IEEE Transactions on Robotics* 28(3):634-649.

[5] Murotsu Y, Senda K, Ozaki M and Tsujio S (1994) Parameter identification of unknown object handled by free-flying space robot. *AIAA journal of guidance, control*, *and dynamics* 17(3):488–494.

[6] Rackl W, Lampariello R and Albu-Schäffer A (2013) Parameter identification methods for free-floating space robots with direct torque sensing. *IFAC proceedings volumes* 46(19):464-469.

[7] Yoshida K and Abiko S (2002) Inertia parameter identification for a free-flying space robot. In: *proceedings of AIAA guidance, navigation, and control conference and exhibit*, p. 4568.

[8] Nguyen-Huynh TC and Sharf I (2013) Adaptive reactionless motion and parameter identification in postcapture of space debris. *AIAA journal of guidance, control*, *and dynamics* 36(2):404–414.

[9] Christidi-Loumpasefski OO, Nanos K and Papadopoulos E (2017) On parameter estimation of space manipulator systems using the angular momentum conservation. In: *proceedings of 2015 IEEE international conference robotics and automation (ICRA)*, Singapore, pp.5453-5458.

[10] Anthony T and Andersen G. (1995) On-orbit modal identification of the Hubble space telescope. *In: proceedings of the american control conference*, Seattle, Washington, USA,1:402-406.

[11] Juang JN and Pappa RS (1984) Galileo spacecraft modal identification using an eigensystem realization algorithm, *NASA AIAA-1984-1070, structures and dynamics division*, NASA Langley Research Center, Hampton, VA, USA, p.1070.

[12] Kasai T, Yamaguchi I, Igawa H, et al. (2009) On-orbit system identification experiments of the Engineering Test Satellite-VIII. *Tr. JSASS Space Tech*; 7: 79–84.

[13] Chamberlain, M.K., Kiefer, S.H., and Banik, J.A. (2018) On-orbit structural dynamics performance of the Roll-Out Solar Array. *In: proceedings of 4th AIAA spacecraft structures conference*, Orlando, FL.

[14] Dodge F.T (2000) The New Dynamic behavior of liquids in moving containers, *Southwest Research Institute.*

[15] Rackl W and Lampariello R (2014) Parameter identification of free-floating robots with flexible appendages and fuel sloshing. In: *proceedings of international conference on modelling, identification & control.*

[16] Green S, Burkey R, Viana F and Sudermann J (2007) Fluid sloshing characteristics in spacecraft propellant tanks with diaphragms. In: *proceedings of 43rd AIAA/ASME/SAE/ASEE joint propulsion conference & exhibit*, Cincinnati, OH.

[17] de Souza AG, de Souza Luiz CG (2015) Design of satellite attitude control system considering the interaction between fuel slosh and flexible dynamics during the system parameters estimation. *applied mechanics and materials* 706:14-24.

[18] Christidi-Loumpasefski OO, Ntinos Ch., and Papadopoulos E (2017) Analytical and experimental parameter estimation for free-floating space manipulator systems. In: *proceedings of 2017 ASTRA*, Leiden, The Netherlands.